

# Orientationally Ordered C<sub>60</sub> on *p*-Sexiphenyl Nanostripes on Ag(111)

Wei Chen,<sup>†,\*</sup> Hongliang Zhang,<sup>†</sup> Han Huang,<sup>‡</sup> Lan Chen,<sup>‡</sup> and Andrew Thye Shen Wee<sup>†,\*</sup>

<sup>†</sup>Department of Physics, National University of Singapore, 2 Science Drive 3, 117542, Singapore, and <sup>‡</sup>Nanoscience and Nanotechnology Initiative, National University of Singapore, 2 Science Drive 3, 117542, Singapore

The controlled assembly of molecules into organic thin films with well-defined supramolecular arrangements on surfaces represents a major challenge, with potential applications in the field of organic electronic devices,<sup>1–9</sup> encompassing organic thin film transistors (OTFTs), organic light-emitting-diodes (OLEDs), and organic solar cells. Much attention has been recently devoted to understand the out-of-plane orientational ordering of planar  $\pi$ -conjugated molecules on surfaces, which is mainly governed by molecule–substrate interfacial interactions or the electronic structure of substrates.<sup>10–12</sup> For example, by manipulating the surface electronic structure of Si(111), control of the molecular orientation of pentacene thin films has been realized, involving pentacene lying-down on metallic Si(111)-( $\sqrt{3} \times \sqrt{3}$ )Au and standing up on semimetallic Si(111)-(5  $\times$  2)Au.<sup>12</sup> Terminating Au(111) with self-assembled monolayers (SAMs) minimizes the electronic coupling between metal d-bands in Au(111) and extended  $\pi$ -orbitals in the organic overlayer, thereby resulting in the orientation transition of copper(II) phthalocyanine (CuPc) thin films from the lying-down configuration on clean Au(111) to the standing-up configuration on SAMs modified Au(111).<sup>13–15</sup>

The in-plane (azimuthal) orientational ordering of molecular monolayer crucially depends on the strong interfacial interaction between molecules and an interlocking with substrates or directional intermolecular interactions.<sup>16–19</sup> For example, the in-plane triple intermolecular hydrogen bonding between perylene tetracarboxylic diimide (PTCDI) and melamine molecules leads to the formation of the well-ordered 2-dimensional (2D) nanoporous honeycomb supramolecular network on Ag-

**ABSTRACT** Long range orientational ordering within C<sub>60</sub> monolayers is observed on *p*-sexithiophene (6P) monolayer nanostripes on Ag(111) at 77 K. Low-temperature scanning tunneling microscopy studies reveal that the C<sub>60</sub>–6P intermolecular interaction constrains all C<sub>60</sub> molecules to adsorb on their hexagons atop 6P molecules. The orientation-dependent bond-to-bond Coulomb interaction between charge deficient single bonds and double bonds with excess charge in neighboring C<sub>60</sub> molecules results in the in-plane orientational ordering and contributes to the lowering of the total energy of the orientationally ordered C<sub>60</sub> islands.

**KEYWORDS:** self-assembly · scanning tunneling microscopy · C<sub>60</sub> · molecular orientation · monolayer

passivated Si(111).<sup>20–23</sup> Fullerene molecular monolayers such as C<sub>60</sub> usually adsorb with random or poorly ordered orientation. Hou, J. G. *et al.* recently reported the formation of two-dimensional (2D) orientationally ordered C<sub>60</sub> domains on self-assembled alkythiols passivated Au(111) at 5 K, which results from a small orientation-dependent bond-to-bond Coulomb energy.<sup>24</sup> Theoretical calculations confirmed that the ground-state of 2D C<sub>60</sub> is a hexagonally closed packed lattice whereby all C<sub>60</sub> molecules have the same orientation.<sup>25</sup> By maximizing the overlap of neighboring molecular orbitals to lower the electron kinetic energy, a novel orientational ordering for potassium (K)-doped C<sub>60</sub> layer has been observed.<sup>26</sup> A complex orientationally ordered C<sub>60</sub> monolayer on Au(111) comprising 49 C<sub>60</sub> molecules in the unit cell mimicking the Si(111)-(7  $\times$  7) reconstruction has been recently reported in a low-temperature scanning tunneling microscopy (LT-STM) study, arising from molecule–substrate interactions as well as intermolecular interactions.<sup>27</sup> All these results suggest that the creation of orientationally ordered molecular thin films can be realized by manipulating the intermolecular and molecule–substrate interfacial interactions.

\*Address correspondence to phycw@nus.edu.sg (W.C.), phyweets@nus.edu.sg (A.T.S.W.).

Received for review January 18, 2008 and accepted March 03, 2008.

Published online March 25, 2008. 10.1021/nn800033z CCC: \$40.75

© 2008 American Chemical Society

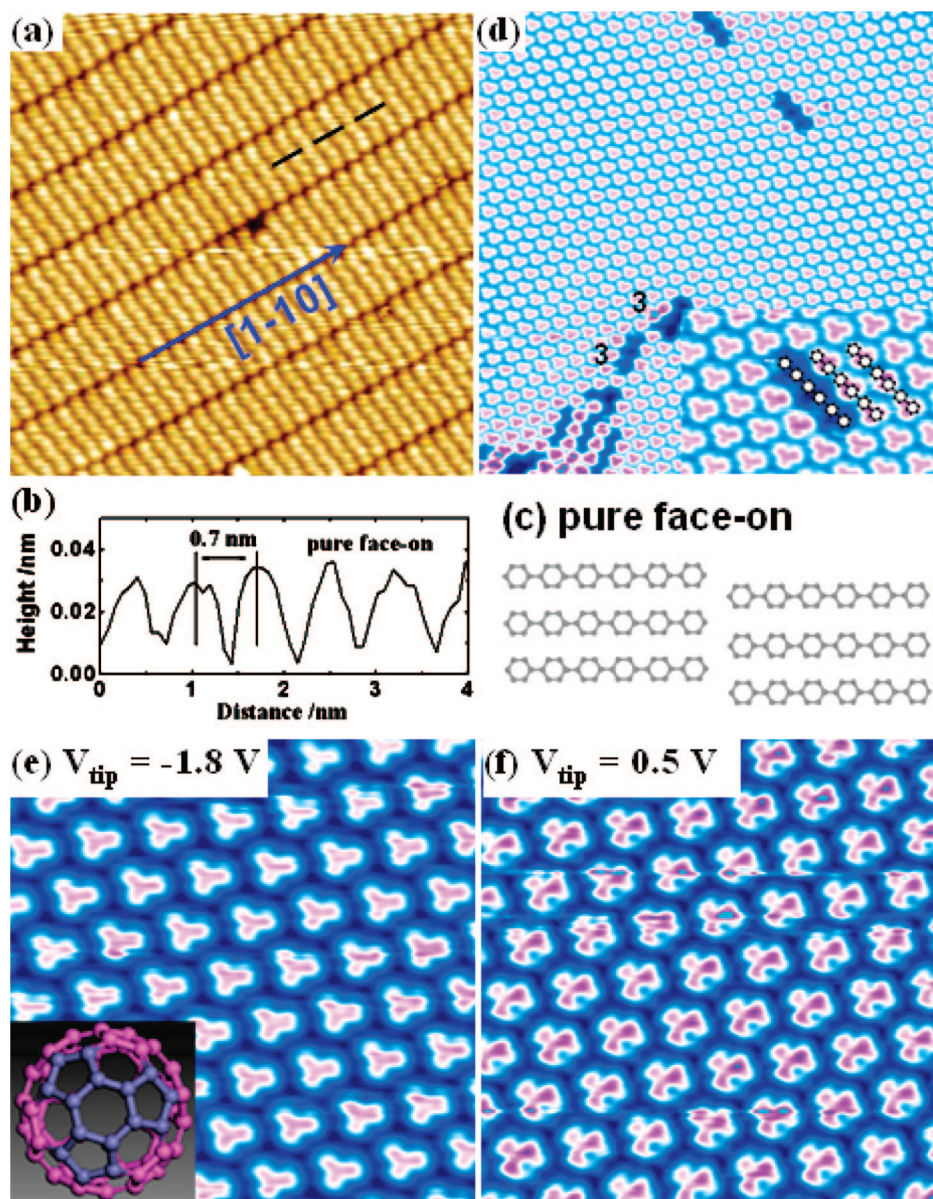


Figure 1. (a) The  $20 \times 20 \text{ nm}^2$  STM image of a "pure face-on" 6P monolayer nanostripe on Ag(111) ( $V_{\text{tip}} = 1.8 \text{ V}$ ); (b) the corresponding line profile as indicated by the dashed line in panel a; (c) the schematic drawing of molecular packing structure for the "pure face-on" 6P nanostripe; (d)  $30 \times 30 \text{ nm}^2$  STM image of orientationally ordered  $\text{C}_{60}$  layer on 6P nanostripes ( $V_{\text{tip}} = -1.8 \text{ V}$ ), the inset showing the corresponding detailed image with the proposed packing structure of the underlying 6P molecules superimposed on the image. (e and f) The  $8 \times 8 \text{ nm}^2$  bias-dependent STM images of the orientationally ordered  $\text{C}_{60}$  layer:  $V_{\text{tip}} = -1.8 \text{ V}$  for panel e and  $V_{\text{tip}} = 0.5 \text{ V}$  for panel f. The inset in panel e shows the cartoon of  $\text{C}_{60}$  with proposed molecular orientation.

In this letter, we report the formation of orientationally ordered  $\text{C}_{60}$  monolayers on *p*-sexithiophene (6P) monolayer nanostripes on Ag(111) at 77 K. It is found that the  $\text{C}_{60}$ –6P intermolecular interaction constrains all  $\text{C}_{60}$  molecules to adsorb on a hexagon. The in-plane orientational ordering arises from the orientation-dependent bond-to-bond Coulomb interaction between neighboring  $\text{C}_{60}$  molecules, lowering the total energy of the  $\text{C}_{60}$  islands.

## RESULTS AND DISCUSSION

Figure 1a shows a  $20 \times 20 \text{ nm}^2$  STM image of 6P monolayer on Ag(111), in which each rodlike bright fea-

ture represents an individual 6P molecule.<sup>29,30</sup> Clearly, the 6P molecules self-assemble via side-by-side packing into highly ordered nanostripe array with a periodicity of  $2.95 \pm 0.02 \text{ nm}$  perpendicular to the chain direction. The line profile in Figure 1b, highlighted by the dashed line in Figure 1a, reveals an intermolecular distance of  $0.70 \pm 0.02 \text{ nm}$  along the chain direction. For 6P in the gas phase or for the isolated 6P molecules on metal surfaces,<sup>31</sup> the adjacent phenyl units within 6P molecules are twisted with respect to each other because of steric hindrance of the hydrogen atoms of neighboring rings. These phenyl ring units become coplanar once 6P molecules form single crystal solids or condensed thin films

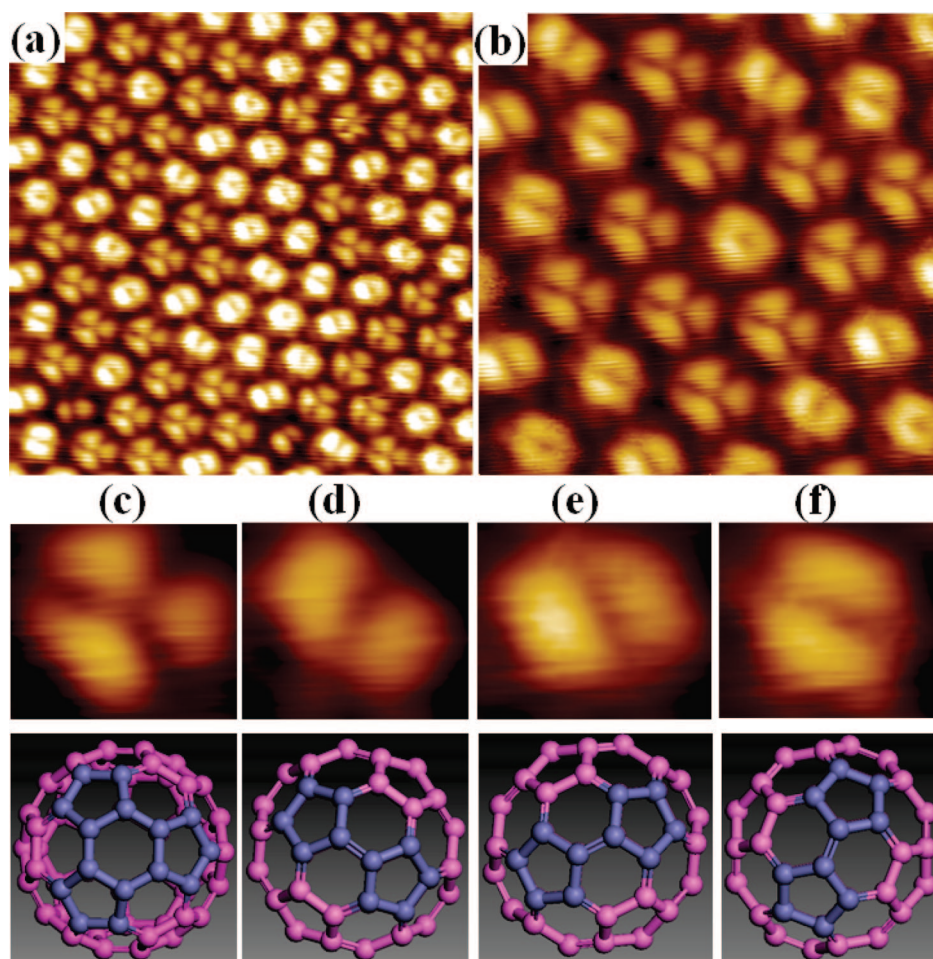


Figure 2. STM images of orientationally disordered  $C_{60}$  monolayer on Ag(111): (a)  $10 \times 10 \text{ nm}^2$ ,  $V_{\text{tip}} = -2.0 \text{ V}$ ; and (b)  $5 \times 5 \text{ nm}^2$ ,  $V_{\text{tip}} = -1.0 \text{ V}$ . Panels c–f show the detailed STM images of  $C_{60}$  with different molecular orientation, and corresponding schematic models are shown below each image.

on substrates.<sup>29,30</sup> The observed 6P molecular packing is very similar to that of  $\alpha$ -sexithiophene on Ag(111) or on the highly ordered pyrolytic graphite (HOPG),<sup>32,33</sup> and is referred to as the “pure face-on” 6P nanostripe phase. Figure 1c displays the schematic drawing of the proposed molecular packing structure.

After depositing 0.5 ML  $C_{60}$  on the “pure face-on” 6P nanostripe template and subsequently annealing at 330 K for 30 min, hexagonally close packed (hcp)  $C_{60}$  single layer islands form on top of the 6P monolayer nanostripes, as shown in Figure 1d. Several  $C_{60}$  vacancy defects are also observed. Most defects correspond to three missing  $C_{60}$  molecules along a close-packed direction, as indicated in Figure 1d. Apparently, all  $C_{60}$  molecules possess 3-fold symmetry, suggesting that the  $C_{60}$  molecules within the islands have the same molecular orientation when imaged at 77 K. Figure 1 panels e and f show the  $8 \times 8 \text{ nm}^2$  bias-dependent STM images of the orientationally ordered  $C_{60}$  layer on 6P nanostripes on Ag(111). The slight difference in STM images arises from the bias-dependent electronic states of  $C_{60}$  molecules. Clearly, all  $C_{60}$  molecules have the same orientation with 3-fold symmetry under different biases, con-

firming our observation of an orientationally ordered  $C_{60}$  layer on 6P nanostripes. It has been reported that the bright lobes in the STM images under negative tip bias or positive sample bias correspond to pentagons of the  $C_{60}$  cage.<sup>27,34,35</sup> The  $C_{60}$  with 3-fold symmetry has been assigned to  $C_{60}$  adsorbed on a hexagon,<sup>27,34</sup> the proposed molecular orientation of which is displayed in the inset in Figure 1e.

In contrast,  $C_{60}$  molecules on clean Ag(111) nucleate into orientationally disordered 2D islands as shown in Figure 2a, which are obtained by room-temperature deposition of  $C_{60}$  on Ag(111) and subsequent annealing at 400 K. The bright–dim STM contrast of  $C_{60}$  molecules in the monolayer can be clearly observed, which was previously proposed to arise from the different coupling of  $C_{60}$  molecules with the underlying Ag(111) surface or  $C_{60}$ -induced reconstruction underneath the dim  $C_{60}$  molecules.<sup>36–43</sup> These  $C_{60}$  molecules exhibit different orientations,<sup>44</sup> as evidenced by the different orientation patterns of  $C_{60}$  in the high resolution STM image in Figure 2b. The orientation patterns with 3- and 2-fold symmetry dominate the image. Figure 2c highlights the 3-fold orientation pattern of  $C_{60}$  adsorbed on a

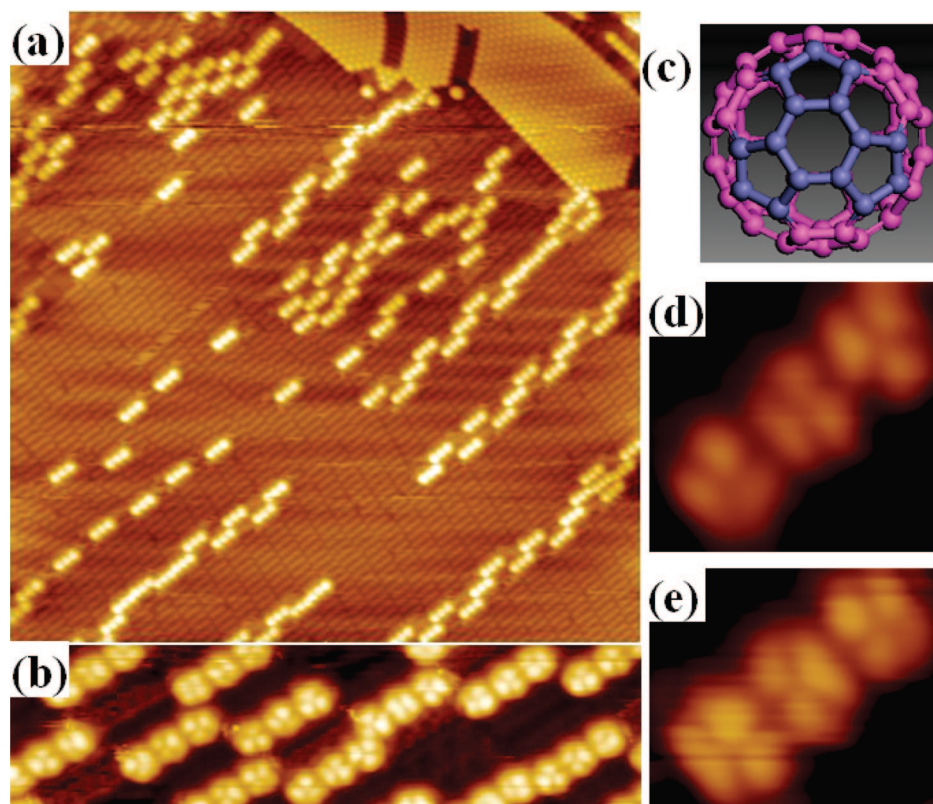


**Figure 3.** (a) The  $80 \times 80 \text{ nm}^2$  STM image near the domain boundary of an orientationally ordered  $\text{C}_{60}$  single island ( $V_{\text{tip}} = 1.8 \text{ V}$ ); (b)  $20 \times 5 \text{ nm}^2$  STM image clearly showing the orientation of  $\text{C}_{60}$  triplets adsorbed on individual 6P molecules ( $V_{\text{tip}} = 1.9 \text{ V}$ ). Panel c displays the schematic model of  $\text{C}_{60}$  adsorbs on a hexagon; panels d and e show the selected  $\text{C}_{60}$  triplets with different molecular orientation.

hexagon with the proposed orientation model shown below. Figure 2 panels d–f highlight the 2-fold orientation patterns with different in-plane rotations, arising from  $\text{C}_{60}$  adsorbing on a double bond in between hexagons (6:6 bond); the corresponding models are shown below each image. Such an orientationally disordered  $\text{C}_{60}$  monolayer is commonly observed on single crystalline metal substrates.<sup>27,44</sup> This suggests that the orientational ordering of  $\text{C}_{60}$  does not rely on strong C–metal interfacial interactions.

Figure 3a displays the  $80 \times 80 \text{ nm}^2$  STM image near the domain boundary of an orientationally ordered  $\text{C}_{60}$  single island, where every three  $\text{C}_{60}$  molecules group together linearly to form a short  $\text{C}_{60}$  molecular rod, which we refer to as a  $\text{C}_{60}$  triplet. The apparent molecular length of 6P ( $\sim 2.95 \text{ nm}$ ) is close to the sum of the diameters of three  $\text{C}_{60}$  molecules ( $1.00 \text{ nm} \times 3 = 3.00 \text{ nm}$ ).<sup>45,46</sup> As such, we propose a model involving the adsorption of a  $\text{C}_{60}$  triplet atop each 6P molecule. These  $\text{C}_{60}$  triplets distribute randomly on the surface. Figure 3b shows the  $20 \times 5 \text{ nm}^2$  STM image revealing the orientation of  $\text{C}_{60}$  triplets adsorbed on individual 6P molecules. Each  $\text{C}_{60}$  molecule possesses the 3-fold symmetric orientation pattern, suggesting that every  $\text{C}_{60}$  molecule adsorbs on a hexagon atop the 6P molecule. The schematic model showing the  $\text{C}_{60}$  orientation is displayed in Figure 3c. We propose that the

preferential adsorption of  $\text{C}_{60}$  triplet on each 6P molecule originates from the donor–acceptor intermolecular interaction or charge transfer between 6P (donor) and  $\text{C}_{60}$  (acceptor). The  $\text{C}_{60}$  molecule adsorbing on a hexagon atop the 6P molecule represents the energetic favorable adsorption geometry of  $\text{C}_{60}$  on 6P. However, more detailed experiments are needed to resolve this hypothesis.

Two selected  $\text{C}_{60}$  triplets are highlighted in Figure 3d,e. Although all the  $\text{C}_{60}$  molecules have the same 3-fold symmetry, the in-plane orientation is rather disordered. Careful inspection of Figure 3b reveals more than 5 different in-plane orientations of the 3-fold symmetric  $\text{C}_{60}$  molecules. This suggests that the 6P– $\text{C}_{60}$  donor–acceptor intermolecular interaction cannot ensure the in-plane orientational ordering of the  $\text{C}_{60}$  monolayer. As shown in Figure 1d,e, all the  $\text{C}_{60}$  molecules within the hcp monolayer on the “pure face-on” 6P nanostripe arrays possess the same 3-fold symmetric orientation pattern and are orientationally ordered. We propose that the 6P– $\text{C}_{60}$  donor–acceptor intermolecular interaction constrains all the  $\text{C}_{60}$  molecules to adsorb on a hexagon atop the 6P molecule. It has been reported that the bond-to-bond Coulomb interaction between charge deficient single bonds and charge excess double bonds of neighboring  $\text{C}_{60}$  molecules depends on the relative  $\text{C}_{60}$  orientations.<sup>34,35,47</sup> This con-

tributes to lowering the total energy of  $C_{60}$  islands and thereby leads to the formation of orientationally ordered  $C_{60}$  domains on self-assembled alkylthiols passivated Au(111) at 5 K. As such, we suggest that such orientation dependent bond-to-bond Coulomb interaction between neighboring  $C_{60}$  molecules controls the in-plane orientational ordering of  $C_{60}$  on 6P nanostripes. The cumulative effects of the 6P– $C_{60}$  donor–acceptor interaction and the orientation dependent bond-to-bond Coulomb interaction lead to the formation of orientationally ordered  $C_{60}$  hcp monolayer on the “pure face-on” 6P nanostripe template. It is worth noting that the underlying 6P layer cannot retain its original nanostripe arrangement due to the  $C_{60}$ –6P interaction resulting in the transition from 2-fold to 3-fold symmetry. 6P molecules are proposed to undergo structural reorganization to accommodate the hcp arrangement of the  $C_{60}$  adlayer.

In conclusion, we have demonstrated the control of the molecular orientational freedom by manipulating the intermolecular and interfacial interactions. LT-STM studies reveal the growth of orientationally ordered hexagonally close-packed  $C_{60}$  monolayer on the “pure

face-on” 6P nanostripe template. The orientational ordering originates from two factors: (i) the 6P– $C_{60}$  donor–acceptor intermolecular interaction which constrains all  $C_{60}$  molecules to adsorb on a hexagon atop 6P molecules; and (ii) the orientation-dependent bond-to-bond Coulomb interaction between charge deficient single bonds and charge excess double bonds of neighboring  $C_{60}$  molecules, which results in the in-plane orientational ordering and contributes to the lowering of the total energy of the orientationally ordered  $C_{60}$  islands. Our present approach provides a feasible process to control the molecular orientational freedom of organic thin films by manipulating the intermolecular and molecule–substrate interfacial interactions. This may have potential applications in organic thin films based OTFTs, OLEDs, and organic solar cells. In particular, a similar process can be easily applied to manipulate the molecular orientation of endohedral fullerenes, which can lead to the possible control of the electronic spin direction inside the fullerene cage, thereby facilitating the design and construction of fullerene-based solid state quantum computers.<sup>48</sup>

## EXPERIMENTAL SECTION

The STM experiments were conducted with an Omicron low-temperature scanning tunneling microscope (LT-STM) housed in a multichamber UHV system with a base pressure better than  $5.0 \times 10^{-11}$  mbar and interfaced to a Nanonis controller (Nanonis, Switzerland).<sup>32,33,49</sup> All STM imaging were performed at 77 K. A clean Ag(111) surface with large terraces was obtained after a few cycles of  $Ar^+$  ion bombardment and subsequent annealing at 800 K.  $C_{60}$  and *p*-sexiphenyl (6P) molecules were evaporated *in situ* from two separated low-temperature Knudsen cells (MBE-Komponenten, Germany) onto the samples held at room temperature (RT) in the growth chamber. The deposition rates of  $C_{60}$  and 6P were monitored by a quartz-crystal-microbalance (QCM) during evaporation, and were further calibrated by counting the adsorbed molecule coverage in the large-scale LT-STM images at coverage below 1 monolayer (1 monolayer = one full monolayer of hexagonally close packed  $C_{60}$  or the “pure face-on” 6P). In our experiments, all depositions were performed at constant rates of about 0.05 ML/min for  $C_{60}$  and 0.10 ML/min for 6P, respectively. During deposition, the chamber pressure was maintained below  $5.0 \times 10^{-10}$  mbar.

**Acknowledgment.** W. Chen acknowledges the financial support by LKY PDF fellowship. The authors acknowledge the support from the A\*STAR Grant R-398-000-036-305 and ARF Grant R-144-000-196-112.

## REFERENCES AND NOTES

- Dimitrakopoulos, C. D.; Malenfant, P. R. L. Organic Thin Film Transistors for Large Area Electronics. *Adv. Mater.* **2002**, *14*, 99–117.
- Sylvester-Hvid, K. O. Two-Dimensional Simulations of CuPc-PCTDA Solar Cells: The Importance of Mobility and Molecular  $\pi$ -Stacking. *J. Phys. Chem. B* **2006**, *110*, 2618–2627.
- de Bettignies, V.; Nicolas, Y.; Blanchard, P.; Levillain, E.; Nunzi, J.-M.; Roncali, J. Planarized Star-Shaped Oligothiophenes as a New Class of Organic Semiconductors for Heterojunction Solar Cells. *Adv. Mater.* **2003**, *15*, 1939–1943.
- Videlot, C.; El Kassmi, A.; Fichou, D. Photovoltaic Properties of Octithiophene-Based Schottky and p/n Junction Cells: Influence of Molecular orientation. *Sol. Energy. Mater. Sol. Cells* **2000**, *63*, 69–82.
- Loi, M. A.; Da Como, E.; Dinelli, F.; Murgia, M.; Zamboni, R.; Biscarini, F.; Muccini, M. Supramolecular Organization in Ultra-thin Films of Alpha-Sexithiophene on Silicon Dioxide. *Nat. Mater.* **2005**, *4*, 81–85.
- Barrena, E.; de Oteyza, D. G.; Sellner, S.; Dosch, H.; Ossó, J. O.; Struth, B. In Situ Study of the Growth of Nanodots in Organic Heteroepitaxy. *Phys. Rev. Lett.* **2006**, *97*, 076102.
- de Oteyza, D. G.; Barrena, E.; Ossó, J. O.; Sellner, S.; Dosch, H. Site-Selective Molecular Organization in Organic Heterostructures. *Chem. Mater.* **2006**, *18*, 4212–4214.
- Oehzelt, M.; Koller, G.; Ivanco, J.; Berkebile, S.; Haber, T.; Resel, R.; Netzer, F. P.; Ramsey, M. G. Organic Heteroepitaxy: *p*-Sexiphenyl on Uniaxially Oriented Alpha-Sexithiophene. *Adv. Mater.* **2006**, *18*, 2466–2470.
- Koller, G.; Berkebile, S.; Krenn, J. R.; Netzer, F. P.; Oehzelt, M.; Haber, T.; Resel, R.; Ramsey, M. G. Heteroepitaxy of Organic - Organic Nanostructures. *Nano. Lett.* **2006**, *6*, 1207–1212.
- Peisert, H.; Schwieger, T.; Auerhammer, J. M.; Knupfer, M.; Golden, M. S.; Fink, J.; Bressler, P. R.; Mast, M. Order on Disorder: Copper Phthalocyanine Thin Films on Technical Substrates. *J. Appl. Phys.* **2001**, *90*, 466–469.
- Kowarik, S.; Gerlach, A.; Sellner, S.; Schreiber, F.; Cavalcanti, L.; Konovalov, O. Real-Time Observation of Structural and Orientational Transitions During Growth of Organic Thin Films. *Phys. Rev. Lett.* **2006**, *96*, 125504.
- Thayer, G. E.; Sadowski, J. T.; zu Heringdorf, F. M.; Sakurai, T.; Tromp, R. M. Role of Surface Electronic Structure in Thin Film Molecular Ordering. *Phys. Rev. Lett.* **2005**, *95*, 256106.
- Chen, W.; Huang, C.; Gao, X. Y.; Wang, L.; Zhen, C. G.; Qi, D. C.; Chen, S.; Zhang, H. L.; Loh, K. P.; Chen, Z. K.; Wee, W. T. S. Tuning the Hole Injection Barrier at the Organic/Metal Interface with Self-Assembled Functionalized Aromatic Thiols. *J. Phys. Chem. B* **2006**, *110*, 26075–26080.

14. Chen, W.; Chen, S.; Qi, D. C.; Gao, X. Y.; Chen, Z. K.; Wee, W. T. S. Surface-Transfer Doping of Organic Semiconductors Using Functionalized Self-Assembled Monolayers. *Adv. Funct. Mater.* **2007**, *17*, 1339–1344.
15. Chen, W.; Wang, L.; Qi, D. C.; Chen, S.; Gao, X. Y.; Wee, A. T. S. Probing the Ultrafast Electron Transfer at the CuPc/Au(111) Interface. *Appl. Phys. Lett.* **2006**, *88*, 184102.
16. Barth, J. V.; Constantini, G.; Kern, K. Engineering Atomic and Molecular Nanostructures at Surfaces. *Nature* **2005**, *437*, 671–679.
17. Rosei, F. Nanostructured Surfaces: Challenges and Frontiers in Nanotechnology. *J. Phys.: Condens. Matter* **2004**, *16*, S1373–S1436.
18. Chen, W.; Wee, A. T. S. Self-Assembly on Silicon Carbide Nanomesh Templates. *J. Phys. D: Appl. Phys.* **2007**, *40*, 6287–6299.
19. Rosei, F.; Schunack, M.; Naitoh, Y.; Jiang, P.; Gourdon, A.; Laegsgaard, E.; Stensgaard, I.; Joachim, C.; Besenbacher, F. Properties of Large Organic Molecules on Metal Surfaces. *Prog. Surf. Sci.* **2003**, *71*, 95–146.
20. Theobald, J. A.; Oxtoby, N. S.; Phillips, M. A.; Champness, N. R.; Beton, P. H. Controlling Molecular Deposition and Layer Structure with Supramolecular Surface Assemblies. *Nature* **2003**, *424*, 1029–1031.
21. Theobald, J. A.; Oxtoby, N. S.; Champness, N. R.; Beton, P. H.; Dennis, T. J. S. Growth Induced Reordering of Fullerene Clusters Trapped in a Two-Dimensional Supramolecular Network. *Langmuir* **2005**, *21*, 2038–2041.
22. Perdigão, L. M. A.; Perkins, E. W.; Ma, J.; Staniec, P. A.; Rogers, B. L.; Champness, N. R.; Beton, P. H. Bimolecular Networks and Supramolecular Traps on Au(111). *J. Phys. Chem. B* **2006**, *110*, 12539–12542.
23. Staniec, P. A.; Perdigão, L. M. A.; Saywell, A.; Champness, N. R.; Beton, P. H. Hierarchical Organisation on a Two-Dimensional Supramolecular Network. *ChemPhysChem* **2007**, *8*, 2177–2181.
24. Hou, J. G.; Yang, J. L.; Wang, H.; Li, Q.; Zeng, C. G.; Yuan, L.; Wang, B.; Chen, D. M.; Zhu, Q. S. Surface Science - Topology of Two-Dimensional C<sub>60</sub> Domains. *Nature* **2001**, *409*, 304–305.
25. Yuan, L. F.; Yang, J. L.; Wang, H. Q.; Zeng, C. G.; Li, Q. X.; Wang, B.; Hou, J. G.; Zhu, Q. S.; Chen, D. M. Low-Temperature Orientationally Ordered Structures of Two-Dimensional C<sub>60</sub>. *J. Am. Chem. Soc.* **2003**, *125*, 169–172.
26. Wang, Y. Y.; Yamachika, R.; Wachowiak, A.; Grobis, M.; Khoo, K. H.; Lee, D.-H.; Louie, S. G.; Crommie, M. F. Novel Orientationally Ordered and Reentrant Metallicity in KxC<sub>60</sub> Monolayers for 3 ≤ x ≤ 5. *Phys. Rev. Lett.* **2007**, *99*, 086402.
27. Schull, G.; Berndt, R. Orientationally Ordered (7 × 7) Superstructure of C<sub>60</sub> on Au(111). *Phys. Rev. Lett.* **2007**, *99*, 226105.
28. France, C. B.; Frame, F. A.; Parkinson, B. A. Multiple Two-Dimensional Structures Formed at Monolayer and Submonolayer Coverages of p-Sexiphenyl on the Au(111) Surface. *Langmuir* **2006**, *22*, 7507–7511.
29. France, C. B.; Parkinson, B. A. Physical and Electronic Structure of p-Sexiphenyl on Au(111). *Appl. Phys. Lett.* **2003**, *82*, 1194–1196.
30. Koller, G.; Berkebile, S.; Oehzelt, M.; Puschnig, P.; Ambrosch-Draxl, C.; Netzer, F. P.; Ramsey, M. G. Intra- and Intermolecular Band Dispersion in an Organic Crystal. *Science* **2007**, *317*, 351–355.
31. Hla, S. W.; Braun, K. F.; Wassermann, B.; Rieder, K. H. Controlled Low-Temperature Molecular Manipulation of Sexiphenyl Molecules on Ag(111) Using Scanning Tunneling Microscopy. *Phys. Rev. Lett.* **2004**, *93*, 208302.
32. Zhang, H. L.; Chen, W.; Chen, L.; Huang, H.; Wang, X. S.; Yuhara, J.; Wee, A. T. S. C<sub>60</sub> Molecular Chains on α-Sexithiophene Nanostripes. *Small* **2007**, *3*, 2015–2018.
33. Huang, H.; Chen, W.; Chen, L.; Zhang, H. L.; Wang, X. S.; Bao, S. N.; Wee, A. T. S. “Zigzag” C<sub>60</sub> Chain Arrays. *Appl. Phys. Lett.* **2008**, *92*, 023105.
34. Wang, H.; Zeng, C.; Wang, B.; Hou, J. G.; Li, Q.; Yang, J. Orientationally Ordered Configurations of the C<sub>60</sub> Molecules in the (2 × 2) Superlattice on a Solid C<sub>60</sub>(111) Surface at Low Temperature. *Phys. Rev. B* **2001**, *63*, 085417.
35. Hou, J. G.; Yang, J. L.; Wang, H. Q.; Li, Q. X.; Zeng, C. G.; Lin, H.; Wang, B.; Chen, D. M.; Zhu, Q. S. Identifying Molecular Orientation of Individual C<sub>60</sub> on a Si(111)-(7 × 7) Surface. *Phys. Rev. Lett.* **1999**, *83*, 3001–3004.
36. Pai, W. W.; Hsu, C.-L.; Lin, M. C.; Lin, K. C.; Tang, T. B. Structural Relaxation of Adlayers in the Presence of Adsorbate-Induced Reconstruction: C<sub>60</sub>/Cu(111). *Phys. Rev. B* **2004**, *69*, 125405.
37. Pai, W. W.; Hsu, C.-L.; Chiang, C. R.; Chang, Y.; Lin, K. C. Origin of Peculiar STM Molecular Contrast in C<sub>60</sub>/Ag(100). *Surf. Sci.* **2002**, *519*, L605–L610.
38. Hsu, C.-L.; Pai, W. W. Aperiodic Incommensurate Phase of a C<sub>60</sub> Monolayer on Ag(100). *Phys. Rev. B* **2003**, *68*, 245414.
39. Pai, W. W.; Hsu, C.-L. Ordering of an Incommensurate Molecular Layer with Adsorbate-Induced Reconstruction: C<sub>60</sub>/Ag(100). *Phys. Rev. B* **2003**, *68*, 121403.
40. Murray, P. W.; Pedersen, M. O.; Lægsgaard, E.; Stensgaard, I.; Besenbacher, F. Growth of C<sub>60</sub> on Cu(110) and Ni(110) Surfaces: C<sub>60</sub>-Induced Interfacial Roughening. *Phys. Rev. B* **1997**, *55*, 9360–9363.
41. Zhang, X.; He, W.; Zhao, A. D.; Li, H. N.; Chen, L.; Pai, W. W.; Hou, J. G.; Loy, M. M. T.; Yang, J. L.; Xiao, X. D. Geometric and Electronic Structure of a C<sub>60</sub> Monolayer on Ag(100). *Phys. Rev. B* **2007**, *75*, 235444.
42. Wang, H. Q.; Hou, J. G.; Takeuchi, O.; Fujisaku, Y.; Kawazu, A. STM Observations of Ag-Induced Reconstruction of C<sub>60</sub> Thin Films. *Phys. Rev. B* **2000**, *61*, 2199–2203.
43. Chen, W.; Zhang, H. L.; Xu, H.; Tok, E. S.; Loh, K. P.; Wee, A. T. S. C<sub>60</sub> on SiC Nanomesh. *J. Phys. Chem. B* **2006**, *110*, 21873–21881.
44. Lu, X. H.; Grobis, M.; Khoo, K. H.; Louie, S. G.; Crommie, M. F. Spatially Mapping the Spectral Density of a Single C<sub>60</sub> Molecule. *Phys. Rev. Lett.* **2003**, *90*, 096802.
45. Heiney, P. A.; Fischer, J. E.; McGhie, A. R.; Romanow, W. J.; Denenstein, A. M.; McCauley, J. P.; Smith, A. B.; Cox, D. E. Orientationally Ordered Transition in Solid C<sub>60</sub>. *Phys. Rev. Lett.* **1991**, *66*, 2911–2914.
46. Altman, E. I.; Colton, R. J. Determination of the Orientation of C<sub>60</sub> Adsorbed on Au(111) and Ag(111). *Phys. Rev. B* **1993**, *48*, 18244–18249.
47. Lu, J. P.; Li, X. P.; Martin, R. M. Ground-State and Phase-Transitions in Solid C<sub>60</sub>. *Phys. Rev. Lett.* **1992**, *68*, 1551–1554.
48. Benjamin, S. C.; Ardavan, A.; Briggs, G. A. D.; Britz, D. A.; Gunlycke, D.; Jefferson, J.; Jones, M. A. G.; Leigh, D. F.; Lovett, B. W.; Khlobystov, A. N.; et al. Towards a Fullerene-Based Quantum Computer. *J. Phys.: Condens. Matter* **2006**, *18*, S867–S883.
49. Chen, W.; Huang, H.; Chen, S.; Chen, L.; Zhang, H. L.; Gao, X. Y.; Wee, A. T. S. Molecular Orientation of 3,4,9,10-Perylene-tetracarboxylic-dianhydride Thin Films at Organic Heterojunction Interfaces. *Appl. Phys. Lett.* **2007**, *91*, 114102.